

Transverse collisional instabilities of a Bose-Einstein condensate in a driven one-dimensional lattice

Sayan Choudhury* and Erich J. Mueller†

Laboratory of Atomic and Solid State Physics, Cornell University, Ithaca, New York 14850, USA

(Received 16 October 2014; published 24 February 2015)

Motivated by recent experiments, we analyze the stability of a three-dimensional Bose-Einstein condensate loaded in a periodically driven one-dimensional optical lattice. Such periodically driven systems do not have a thermodynamic ground state but may have a long-lived steady state which is an eigenstate of a “Floquet Hamiltonian.” We explore collisional instabilities of the Floquet ground state which transfer energy into the transverse modes. We calculate decay rates, finding that the lifetime scales as the inverse square of the scattering length and inverse of the peak three-dimensional density. These rates can be controlled by adding additional transverse potentials.

DOI: [10.1103/PhysRevA.91.023624](https://doi.org/10.1103/PhysRevA.91.023624)

PACS number(s): 67.85.Hj, 03.75.-b

I. INTRODUCTION

In recent years, rapid progress has been made in quantum simulation, whereby one engineers a quantum system to study important phenomena experimentally [1–5]. Periodically driven quantum systems (Floquet systems) are a particularly versatile platform for such simulations [6,7] and have already been used to explore a variety of rich physics. This program has been particularly successful in cold atoms, where periodic driving has been integral to studying models of classical frustrated magnetism, and models of topological matter [8–21]. These periodically driven systems have seen extensive theoretical modeling [22–55]. Some of these experiments have experienced unexpected heating [16]. In an earlier paper, we began addressing the sources of this heating by studying collisions within a one-dimensional Bose-Einstein condensate (BEC) in a shaken optical lattice [56]. We found that, in the presence of strong transverse confinement, interactions can drive instabilities but that there were large parameter ranges where the system was stable. Here we extend that work to the regime where there is no transverse confinement. The additional decay channels generally lead to more dissipation and diffusive dynamics.

In this paper, we consider two paradigmatic examples of Floquet systems in which a three-dimensional BEC is loaded into a modulated one-dimensional lattice. The difference lies in the nature of the drive: We consider (a) amplitude modulation of lattice depth (similar to the setup in Refs. [17–19]) and (b) lattice shaking (similar to the setup in Refs. [20,21]). These two protocols are illustrated schematically in Fig. 1. We solve the Schrödinger equation for both systems and treat the interatomic interactions perturbatively. Our analysis is along the lines of Ref. [56], where we used Fermi’s golden rule to study the tight confinement limit. This kinetic approach can be contrasted with quantum coherent arguments such as those used by Creffield [57]. Creffield used the Bogoliubov equations to look at a dynamical instability of a BEC in a shaken one-dimensional optical lattice. These decay channels are important when the interactions are strong. We consider a different limit: for most recent experiments, the interaction strengths are too low for the interaction-driven modification of

the dispersion to be relevant; rather, the physics is dominated by the energy- and momentum-conserving scattering processes which are accounted for through our kinetic equations. In a field-theoretic formulation this corresponds to keeping only the imaginary part of the self-energy.

In Sec. II, we analyze the stability of a BEC in an amplitude-modulated tilted optical lattice. A similar analysis can be used for Raman-driven lattices, such as those used to realize the Harper Hamiltonian [16,19]. It also applies to the study of density-induced tunneling [58] and is related to earlier studies of Bloch oscillations [59]. In Sec. III, we study the stability of a BEC loaded in a shaken optical lattice. This system can be mapped onto a classical spin model which exhibits a paramagnetic-ferromagnetic phase transition as well as a roton-maxon excitation spectrum [20,21]. In both Secs. II and III, we obtain analytical results for the lifetime of the BEC. Finally, in Sec. IV, we discuss the general form of the dissipation rate in driven systems.

II. AMPLITUDE-MODULATED LATTICE

In this section, we consider a BEC in a deep tilted one-dimensional optical lattice. Adjacent sites are offset by an energy $\Delta \gg J$, suppressing tunneling (with J being the nearest-neighbor tunneling matrix element). There is no transverse confinement, yielding a one-dimensional array of pancakes. The lattice depth is then modulated at a frequency ω ($\approx \Delta$) so that tunneling is restored between the pancakes. The Hamiltonian describing this system is

$$H = \int d^2r_\perp \sum_j -[J + 2\Omega \cos(\omega t)](a_{j+1}^\dagger a_j + a_j^\dagger a_{j+1}) + \Delta j a_j^\dagger a_j + \frac{\bar{g}}{2} a_j^\dagger a_j^\dagger a_j a_j + \frac{\hbar^2}{2m} \nabla_\perp a_j^\dagger \nabla_\perp a_j. \quad (1)$$

The constant Ω parameterizes the modulation of the hopping matrix element. The transverse spatial components are suppressed: $a_j = a_j(r_\perp)$, where $r_\perp = (x, y)$ and $\nabla_\perp = \hat{x}\partial_x + \hat{y}\partial_y$. The coupling constant is

$$\begin{aligned} \bar{g} &= \frac{4\pi\hbar^2 a_s}{m} \int dz \phi(z)^4 \\ &= \frac{4\pi\hbar^2 a_s}{md}, \end{aligned} \quad (2)$$

*sc2385@cornell.edu

†em256@cornell.edu

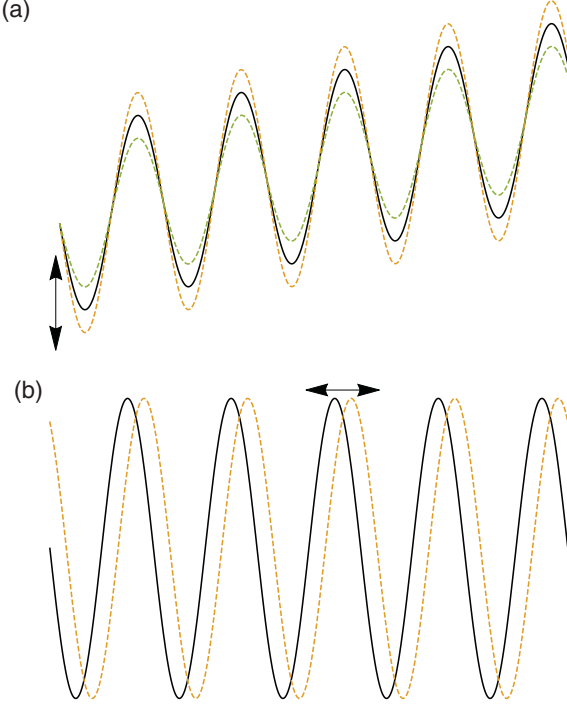


FIG. 1. (Color online) The two protocols of lattice driving: (a) an amplitude-modulated tilted lattice and (b) a shaken lattice.

where $\phi(z)$ is the Wannier wave function in the z direction, normalized so that $\int |\phi|^2 dz = 1$ and a is the lattice spacing. This equation defines d , the size of the Wannier state, and is valid if $d \gg a_s$ [60].

Depending on how one sets up the problem, the $\phi(z)$ used in Eq. (2) will be either the Wannier states of the static lattice, some time average of the instantaneous eigenstates, or even some time-dependent function which yields an oscillating \bar{g} . The distinction will be important if the drive frequency is resonant with a band-changing collision or if the modulation amplitude is large. Similarly, the relationship between J, Ω , and the lattice parameters may be renormalized by large-amplitude driving, and the time dependence of the parameters may not be sinusoidal. For most present experiments, where the amplitude of oscillations is small, these effects can be ignored.

As in [61], we now perform a gauge transformation to replace the tilt with a time-dependent phase:

$$a_j = b_j e^{-i\Delta jt}. \quad (3)$$

The operators b_j will evolve with a new Hamiltonian H' , chosen so that

$$i\partial_t b_j = [b_j, H']. \quad (4)$$

Specializing to the resonant case $\omega = \Delta$, we Fourier transform this equation, yielding

$$H' = \sum_k \epsilon_k(t) b_k^\dagger b_k + \frac{g}{2V} \sum_{\mathbf{k}_1, \mathbf{k}_2, \mathbf{k}_3} b_{\mathbf{k}_1}^\dagger b_{\mathbf{k}_2}^\dagger b_{\mathbf{k}_3} b_{\mathbf{k}_4}, \quad (5)$$

where $\mathbf{k}_4 = \mathbf{k}_1 + \mathbf{k}_2 - \mathbf{k}_3$, $\mathbf{k} = \{k_z, k_\perp\}$, and $g = \bar{g}a$, where a is the lattice spacing. The instantaneous single-particle

dispersion is given by

$$\begin{aligned} \epsilon_{\mathbf{k}}(t) = & -2\Omega \cos(k_z) - 2\Omega \cos(k_z - 2\Delta t) \\ & - 2J \cos(k_z - \Delta t) + \frac{\hbar^2 k_\perp^2}{2m}, \end{aligned} \quad (6)$$

where V is the system volume and $b_{\mathbf{k}} = \sum_j b_j \exp(i\mathbf{k}j)$. The best interpretation of this dispersion comes from looking at the group velocity of a wave packet, $\partial\epsilon/\partial k$. There is a drift term $v_d = \partial\epsilon/\partial k_z = 2\Omega \sin(k_z)$ and an oscillating part $v_m = \partial\epsilon/\partial k_z = -4\Omega\Delta \sin(k_z - 2\Delta t) - 2J \sin(k_z - \Delta t)$, which is analogous to micromotion in ion traps [62].

We wish to explore the behavior of a condensate at $\mathbf{k} = 0$. To this end, we break our Hamiltonian into three terms $H' = H_0 + H_1 + H_2$,

$$H_0 = \sum_{\mathbf{k}} \epsilon_{\mathbf{k}}(t) b_{\mathbf{k}}^\dagger b_{\mathbf{k}} + \frac{g}{2V} b_0^\dagger b_0^\dagger b_0 b_0 + \frac{2g}{V} \sum_{\mathbf{k} \neq 0} b_0^\dagger b_{\mathbf{k}}^\dagger b_{\mathbf{k}} b_0, \quad (7)$$

$$H_1 = \alpha \frac{g}{2V} \sum_{\mathbf{k} \neq 0} b_{-\mathbf{k}}^\dagger b_{\mathbf{k}}^\dagger b_0 b_0 + \text{H.c.}, \quad (8)$$

$$H_2 = H - H_1 - H_0, \quad (9)$$

where $\alpha = 1$ is a formal parameter we will use for perturbation theory. As α is accompanied by a factor of the interaction strength gN/V , this expansion is equivalent to perturbation theory in g . Here H_0 contains the single-particle physics and the Hartree-Fock terms, H_1 contains interaction terms corresponding to atoms scattering from the condensate to finite-momentum states, and H_2 contains terms where a condensed atom and a noncondensed atom scatter or two noncondensed atoms scatter. H_2 does not contribute at the lowest order in perturbation theory, as there are initially no noncondensed atoms.

We will imagine that at time $t = 0$ we are in the state

$$|0\rangle = \frac{(b_0^\dagger)^N}{\sqrt{N!}} |\text{vac}\rangle, \quad (10)$$

which is an eigenstate of H_0 . We will perturbatively calculate how $|\psi(t)\rangle$ evolves. To lowest order,

$$|\psi(t)\rangle = e^{-i\frac{E_0 t}{\hbar}} \left[|0\rangle + \sum_{\mathbf{k}} c_{\mathbf{k}}(t) |\mathbf{k}\rangle + \dots \right], \quad (11)$$

where the state $|\mathbf{k}\rangle$ is given by

$$|\mathbf{k}\rangle = b_{\mathbf{k}}^\dagger b_{-\mathbf{k}}^\dagger \frac{(b_0^\dagger)^{N-2}}{\sqrt{(N-2)!}} |\text{vac}\rangle \quad (12)$$

and the coefficient is

$$c_{\mathbf{k}}(t) = \frac{\Lambda_k}{i\hbar} \int_0^t d\tau \exp \left[-i \int_\tau^t 2 \frac{E_k(s)}{\hbar} ds \right], \quad (13)$$

whose amplitude is given by

$$\Lambda_k = \langle \mathbf{k} | H_1 | 0 \rangle / \alpha = \frac{gn}{2}. \quad (14)$$

In Eq. (13), the (Hartree-Fock) excitation energy is

$$E_k(t) = \epsilon_{\mathbf{k}}(t) + gn - \epsilon_0(t). \quad (15)$$

Performing the integral in the exponent yields

$$\begin{aligned} \int_{\tau}^t E_k(s) ds &= E_k^{(0)}(t - \tau) \\ &+ \frac{\Omega}{\Delta} [\sin(k_z - 2\Delta\tau) - \sin(k_z - 2\Delta t)] \\ &+ \frac{2J}{\Delta} [\sin(k_z - \Delta\tau) - \sin(k_z - \Delta t)], \end{aligned} \quad (16)$$

where the “effective dispersion” is

$$E_k^{(0)} = 2\Omega[1 - \cos(k_z)] + gn + \frac{k_{\perp}^2}{2m}. \quad (17)$$

This energy corresponds to the spectrum one would obtain from Floquet theory. It takes the form of a tight-binding model along z with a nearest-neighbor hopping of strength Ω . The resonant modulation has restored hopping. We now expand Eq. (13) in powers of J/Δ and Ω/Δ . Neglecting off-resonant terms and making the standard approximation $\sin^2(xt)/(xt)^2 \approx 2\pi t \delta(x)$, we find

$$\begin{aligned} |c_{\mathbf{k}}|^2 &\approx \frac{|\Lambda_k|^2}{\hbar} \frac{\Omega^2}{\Delta^2} t 2\pi \delta(E_k^{(0)} - \Delta) \\ &+ \frac{|\Lambda_k|^2}{\hbar} \frac{4J^2}{\Delta^2} t 2\pi \delta(E_k^{(0)} - \Delta/2), \end{aligned} \quad (18)$$

which is analogous to Fermi’s golden rule. The result can also be derived using the formulation in Ref. [63]. The first term proportional to Ω^2 is naturally interpreted as coming from a pair of particles absorbing a lattice vibration. The second term involves one particle “hopping downhill” with the potential energy converted to transverse motion.

We now calculate the total rate of scattering out of the condensate. The relevant time scale is

$$\begin{aligned} \frac{1}{\tau} &= \frac{1}{N_0} \partial_t N_0 = \frac{2}{N} \partial_t \sum_k |c_{\mathbf{k}}|^2 \\ &= \frac{1}{\tau_2} + \frac{1}{\tau_1}, \end{aligned} \quad (19)$$

$$\frac{1}{\tau_2} = \frac{2|\Lambda_k|^2}{N\hbar} \frac{\Omega^2}{\Delta^2} \sum_k 2\pi \delta(E_k^{(0)} - \Delta),$$

$$\frac{1}{\tau_1} = \frac{2|\Lambda_k|^2}{N\hbar} \frac{4J^2}{\Delta^2} \sum_k 2\pi \delta(E_k^{(0)} - \Delta/2). \quad (20)$$

The sums over k are straightforward. We first note that because Ω is small, the dependence of $E_k^{(0)}$ on k_z is weak and can be neglected. Thus the sum over k just yields a constant

$$\begin{aligned} \rho(v) &= \sum_k 2\pi \delta(E_k^{(0)} - v) \\ &\approx \frac{V}{a} \int \frac{d^2 k_{\perp}}{(2\pi)^2} 2\pi \delta\left(\frac{k_{\perp}^2}{2m} + gn - v\right) \\ &= \frac{Vm}{a}. \end{aligned} \quad (21)$$

Putting in the factors of \hbar , the total rate of scattering out of the condensate is

$$\begin{aligned} \frac{1}{\tau} &= \frac{g^2 nm}{2a\hbar^3} \frac{\Omega^2 + 4J^2}{\Delta^2} \\ &= gn \frac{2\pi a_s}{\hbar d} \frac{\Omega^2 + 4J^2}{\Delta^2}. \end{aligned} \quad (22)$$

Some typical numbers are $gn/h \sim 300$ Hz, $\Omega \sim 40$ Hz, $J \sim 5$ Hz, $\Delta \sim 1$ kHz, and $d \sim 75$ nm. For ^{87}Rb , the scattering length is $a_s \sim 5$ nm. Thus the lifetime of the BEC is about 750 ms.

III. SHAKEN LATTICE

In this section, we look at the stability of a three-dimensional BEC loaded into a shaken one-dimensional optical lattice. We considered the strictly one-dimensional version in Ref. [56]. We are motivated by the setup in Ref. [21], where Ha *et al.* load a three-dimensional BEC of ^{133}Cs atoms in a one-dimensional lattice and then shake the lattice at a frequency resonant with the zero-energy band gap of the first two bands. This results in a strong mixing of the first two bands (schematically illustrated in Fig. 2). For our analysis,

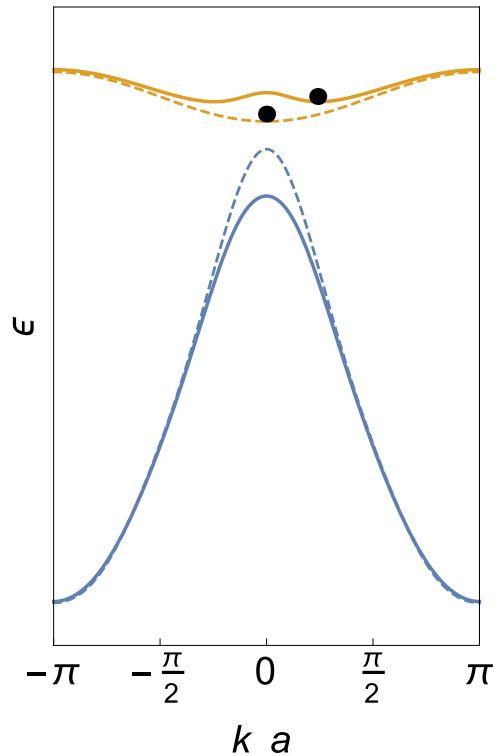


FIG. 2. (Color online) Schematic showing first (top) and second (bottom) Floquet quasienergy bands of an optical lattice: ϵ is the single-particle energy, k is the quasimomentum, and a is the lattice spacing. Since Floquet energies are only defined modulo the shaking quanta $\hbar\omega$, the energy of the second band has been shifted down by $\hbar\omega$. Alternatively, this shift can be interpreted as working in a dressed basis, where the energy includes a contribution from the phonons. The mixing between the bands depends on the shaking amplitude. Dashed curves correspond to weak shaking, where the first band has its minimum at $k = 0$. Solid curves correspond to strong shaking, where there are two minima at $k = \pm k_0 \neq 0$.

we label the Bloch band connected adiabatically to the first Bloch band in the limit of zero shaking as the ground band. As is evident from Fig. 2, due to level repulsion between the Bloch bands, the ground band exhibits a bifurcation from having one minimum at $\{\mathbf{k} = 0\}$ to two minima at $\{\mathbf{k}_\perp = 0, k = k_0 \neq 0\}$. This is analogous to the paramagnetic-ferromagnetic phase transition in Landau theory for classical spin models. In the paramagnetic regime the bosons always condense at $\mathbf{k} = 0$, while in the ferromagnetic regime, the bosons condense at some finite momentum $\{\mathbf{k}_\perp = 0, k \neq 0\}$. Here we first perturbatively analyze the stability of a BEC against collisions in the limit of weak forcing amplitude. This gives an intuitive picture about how the scattering rate varies with amplitude. We then numerically calculate collision rates for larger shaking amplitudes spanning the experimentally interesting critical region. We find that the linearized theory overestimates the damping but gives the correct order of magnitude.

A. Model

In the frame comoving with the lattice, the tight-binding Hamiltonian describing the system can be written as $H_0(t) + H_{\text{int}}$:

$$\begin{aligned} H_0(t) &= \int d^2 r_\perp \sum_{ij} \left(-t_{ij}^{(1)} a_i^\dagger a_j + t_{ij}^{(2)} b_i^\dagger b_j + \text{H.c.} \right) \\ &\quad + \sum_j F \cos(\omega t) [z_j (a_j^\dagger a_j + b_j^\dagger b_j) + \chi_j a_j^\dagger b_j \\ &\quad + \chi_j^* b_j^\dagger a_j] + \frac{\hbar^2}{2m} (\nabla_\perp a_j^\dagger \nabla_\perp a_j + \nabla_\perp b_j^\dagger \nabla_\perp b_j), \end{aligned} \quad (23)$$

$$\begin{aligned} H_{\text{int}} &= \int d^2 r_\perp \sum_i \frac{\bar{g}_1}{2} a_i^\dagger a_i^\dagger a_i a_i + \frac{\bar{g}_2}{2} b_i^\dagger b_i^\dagger b_i b_i \\ &\quad + 2\bar{g}_{12} a_i^\dagger b_i^\dagger a_i b_i + H', \end{aligned} \quad (24)$$

where

$$\begin{aligned} \chi_j &= \int dz z w_1^*(z - z_j) w_2(z - z_j), \\ t_{ij}^{(1)} &= \int dz w_1^*(z - z_i) \left(\frac{-\hbar^2}{2m} \frac{d^2}{dz^2} + V(z) \right) w_1^*(z - z_j), \\ t_{ij}^{(2)} &= \int dz w_2^*(z - z_i) \left(\frac{-\hbar^2}{2m} \frac{d^2}{dz^2} + V(z) \right) w_2^*(z - z_j), \end{aligned}$$

with $V(z) = V_0 \sin^2(\frac{2\pi z}{\lambda_L})$ and H' being off-resonant. It should also be noted that χ_j is independent of j , so we can call it χ . If necessary, more bands can be included.

We now perform a basis rotation: $|\psi\rangle \rightarrow U_c(t)|\psi\rangle$ with

$$U_c(t) = \exp \left(-\frac{i}{\hbar} \int_0^t \sum_j z_j F_0 \cos(\omega t) (a_j^\dagger a_j + b_j^\dagger b_j) dt \right). \quad (25)$$

Under this unitary transformation, the Hamiltonian becomes

$$\begin{aligned} H'_0(t) &= U_c H_0(t) U_c^{-1} - i\hbar U_c \partial_t U_c^{-1} \\ &= \sum_{ij} \left[-J_{ij}^{(1)}(t) a_i^\dagger a_j + J_{ij}^{(2)}(t) b_i^\dagger b_j + \text{H.c.} \right] \end{aligned}$$

$$\begin{aligned} &+ \sum_j F \cos(\omega t) (\chi a_j^\dagger b_j + \chi^* b_j^\dagger a_j) + \sum_{k_\perp} \frac{\hbar^2 k_\perp^2}{2m} \\ &= \sum_k \sum_m \cos(mka) \left[-J_m^{(1)}(t) a_k^\dagger a_k - J_m^{(2)}(t) b_k^\dagger b_k \right] \\ &+ \sum_k F_0 \cos(\omega t) (\chi a_k^\dagger b_k + \chi^* b_k^\dagger a_k) + \sum_{k_\perp} \frac{\hbar^2 k_\perp^2}{2m}, \end{aligned} \quad (26)$$

where

$$\begin{aligned} J_{ij}^\sigma(t) &= t_{ij}^\sigma \exp \left[-i F_0 \frac{\cos(\omega t)}{\hbar\omega} (z_i - z_j) \right] \\ &= t_{ij}^\sigma \exp \left[-i F_0 \frac{\cos(\omega t)}{\hbar\omega} a(i - j) \right], \end{aligned} \quad (27)$$

$a = \lambda_L/2$ is the lattice spacing, and $\chi = \chi^*$ for a suitable choice of phase for a_k and b_k .

Thus, in the limit of $F/(\hbar\omega) \ll 1$, the Hamiltonian describing the system is $H = H_{\text{sp}} + H_{\text{int}}$, where

$$H_{\text{sp}} = \sum_{\mathbf{k}} \epsilon_{\mathbf{k}}^{(1)} a_{\mathbf{k}}^\dagger a_{\mathbf{k}} + \epsilon_{\mathbf{k}}^{(2)} b_{\mathbf{k}}^\dagger b_{\mathbf{k}} + \chi F \cos(\omega t) (a_{\mathbf{k}}^\dagger b_{\mathbf{k}} + b_{\mathbf{k}}^\dagger a_{\mathbf{k}}), \quad (28)$$

$$\begin{aligned} H_{\text{int}} &= \int d^2 r_\perp \sum_i \frac{\bar{g}_1}{2} a_i^\dagger a_i^\dagger a_i a_i + \frac{\bar{g}_2}{2} b_i^\dagger b_i^\dagger b_i b_i \\ &\quad + 2\bar{g}_{12} a_i^\dagger b_i^\dagger a_i b_i + H'. \end{aligned} \quad (29)$$

Here $\epsilon_{\mathbf{k}}^{(1)}$ ($\epsilon_{\mathbf{k}}^{(2)}$) is the dispersion of the first (second) band and $a_{\mathbf{k}}$ ($b_{\mathbf{k}}$) is the annihilation operator for particles in the first (second band).

We make the transformation $b_{\mathbf{k}} \rightarrow \exp(-i\omega t)b_{\mathbf{k}}$ and discard far-off-resonant terms (making the rotating-wave approximation) to simplify the single-particle terms:

$$H_{\text{RWA}}^{(\text{sp})} = \sum_{\mathbf{k}} \epsilon_{\mathbf{k}}^{(1)} a_{\mathbf{k}}^\dagger a_{\mathbf{k}} + \epsilon_{\mathbf{k}}^{(2)} b_{\mathbf{k}}^\dagger b_{\mathbf{k}} + \chi F (a_{\mathbf{k}}^\dagger b_{\mathbf{k}} + b_{\mathbf{k}}^\dagger a_{\mathbf{k}}). \quad (30)$$

Here $\mathbf{k} = \{k, \mathbf{k}_\perp\}$, $\epsilon_{\mathbf{k}}^{(1)} = \epsilon_k^{(1)} + (\hbar k_\perp)^2/(2m)$, $\epsilon_{\mathbf{k}}^{(2)} = \epsilon_k^{(2)} + (\hbar k_\perp)^2/(2m) - \hbar\omega$. We diagonalize this quadratic form, writing

$$H_{\text{RWA}}^{(\text{sp})} = \sum_{\mathbf{k}} \bar{\epsilon}_{\mathbf{k}}^{(1)} \bar{a}_{\mathbf{k}}^\dagger \bar{a}_{\mathbf{k}} + \bar{\epsilon}_{\mathbf{k}}^{(2)} \bar{b}_{\mathbf{k}}^\dagger \bar{b}_{\mathbf{k}}. \quad (31)$$

The dressed dispersions $\bar{\epsilon}_{\mathbf{k}}^{(1)}$ and $\bar{\epsilon}_{\mathbf{k}}^{(2)}$ are shown as solid lines in Fig. 2. The bare dispersions $\epsilon_{\mathbf{k}}^{(1)}$ and $\epsilon_{\mathbf{k}}^{(2)}$ are shown as dashed lines. We treat $H_{\text{RWA}}^{(\text{sp})}$ both perturbatively and nonperturbatively to obtain scattering rates in the next two sections.

B. Perturbation theory

For small forcing amplitudes, we gain insight with a perturbative expansion in F . To linear order in F , the dressed operators are

$$\bar{a}_{\mathbf{k}}^\dagger = a_{\mathbf{k}}^\dagger - (\chi F)/(\epsilon_{\mathbf{k}}^{(2)} - \epsilon_{\mathbf{k}}^{(1)}) b_{\mathbf{k}}^\dagger, \quad (32)$$

$$\bar{b}_{\mathbf{k}}^\dagger = b_{\mathbf{k}}^\dagger + (\chi F)/(\epsilon_{\mathbf{k}}^{(2)} - \epsilon_{\mathbf{k}}^{(1)}) a_{\mathbf{k}}^\dagger. \quad (33)$$

Because we have made the rotating-wave approximation, we have a time-independent problem and can simply apply Fermi's golden rule. The standard procedure yields a scattering rate:

$$\frac{dN}{dt} = \int \frac{dk}{2\pi} \int \frac{d^2 k_\perp}{(2\pi)^2} |\langle \psi_f | H_{\text{int}} | \psi_i \rangle|^2 \sigma, \\ \sigma = \frac{2\pi}{\hbar} \delta \left(\bar{\epsilon}_k^{(1)} + \bar{\epsilon}_k^{(2)} + \frac{(\hbar k_\perp)^2}{m} - 2\bar{\epsilon}_0^{(1)} \right). \quad (34)$$

The initial and final states are

$$|\psi_i\rangle = \frac{(\bar{a}_0^\dagger)^N}{\sqrt{N!}} |0\rangle, \\ |\psi_f\rangle = \bar{b}_{\mathbf{k}}^\dagger \bar{a}_{-\mathbf{k}}^\dagger \frac{(\bar{a}_0^\dagger)^{(N-2)}}{\sqrt{N-2!}} |0\rangle. \quad (35)$$

Here $|\psi_i\rangle$ represents all particles in the condensate, while $|\psi_f\rangle$ has one particle with momentum \mathbf{k} in the dressed b band and one with momentum $-\mathbf{k}$ in the ground band.

The transverse integrals are elementary and yield

$$\frac{dN}{dt} = \frac{m}{2\hbar^3} n^2 \int \frac{dk}{2\pi} \left(\frac{g_1}{\Delta_k} - 2\frac{g_{12}}{\Delta_0} \right)^2 (\chi F)^2, \quad (36)$$

where $\Delta_k = (\epsilon_k^{(2)} - \epsilon_k^{(1)})$, $\Delta_0 = (\epsilon_0^{(2)} - \epsilon_0^{(1)})$, and $g = \bar{g}a$. While Eq. (36) can always be integrated numerically, we have found a sequence of approximations which lets us analytically estimate the scattering rate. First, we approximate the Wannier functions as $w_1(x) = (\frac{1}{d_1^2\pi})^{1/4} \exp(-x^2/2d_1^2)$ and $w_2(x) = (\frac{1}{\pi d_1^2})^{3/4} x \exp(-x^2/2d_1^2)$, where $d_1 = a/[\pi(V_0)^{1/4}]$ (with V_0 being the lattice depth expressed in units of E_R). Within this approximation, $g_1 \approx 2g_{12}$, where $g_1 = (4\pi\hbar^2 a_s a)/(md)$, with $d = d_1\sqrt{2\pi}$ being the size of the Wannier state and a_s being the scattering length. This is a good approximation as a numerical calculation using the exact Wannier states for the lattice in Ref. [20,21] yields $g_1 = (1/0.41) g_{12}$.

As a second approximation, we note that, except for k near 0, $\Delta_k \gg \Delta_0$. The contribution of those parts to the integral in Eq. (36) is small, allowing us to neglect the k dependence of the integrand. Hence we see that the rate of scattering is approximately

$$\frac{dN}{dt} \approx (g_1 n)^2 \left(\frac{\chi F}{\Delta_0} \right)^2 \frac{Vm}{2a\hbar^3}. \quad (37)$$

This gives the time scale for the scattering as

$$\tau = \frac{N}{\frac{dN}{dt}} \approx \frac{2\hbar^3 a}{mg_1^2 n} \left(\frac{\Delta_0}{\chi F} \right)^2. \quad (38)$$

Stronger interactions, higher density, and larger forcing amplitudes all increase the scattering rate.

C. Beyond perturbation theory

In this section, we extend our results to larger F . This allows us to probe the critical and ferromagnetic region. Generically, we write

$$\bar{a}_{\mathbf{k}}^\dagger = u_k a_{\mathbf{k}}^\dagger + v_k b_{\mathbf{k}}^\dagger, \quad (39)$$

$$\bar{b}_{\mathbf{k}}^\dagger = -v_k a_{\mathbf{k}}^\dagger + u_k b_{\mathbf{k}}^\dagger, \quad (40)$$

with $|u_k|^2 + |v_k|^2 = 1$. In particular,

$$u_k = \frac{1}{\sqrt{1 + |\gamma_k|^2}}, \quad v_k = \frac{g_k}{\sqrt{1 + |\gamma_k|^2}}, \\ \frac{1}{\gamma_k} = \frac{\sqrt{4F^2\chi^2 + \delta\epsilon_k^2} + \delta\epsilon_k}{2\chi F}, \\ \delta\epsilon_k = \epsilon_k^{(1)} - \epsilon_k^{(2)}.$$

One can invert the above relationships to obtain

$$a_{\mathbf{k}}^\dagger = u_k \bar{a}_{\mathbf{k}}^\dagger - v_k \bar{b}_{\mathbf{k}}^\dagger, \quad (41)$$

$$b_{\mathbf{k}}^\dagger = v_k \bar{a}_{\mathbf{k}}^\dagger + u_k \bar{b}_{\mathbf{k}}^\dagger. \quad (42)$$

For $F < F_c$ (WITH F_c being the critical shaking force), we use Eq. (35) as our initial and final states. For $F > F_c$, we use

$$|\psi_i\rangle = \frac{(\bar{a}_{\mathbf{k}_0}^\dagger)^N}{\sqrt{N!}} |0\rangle, \\ |\psi_f^{(1)}\rangle = \bar{b}_{\mathbf{k}_0+\mathbf{k}}^\dagger \bar{a}_{\mathbf{k}_0-\mathbf{k}}^\dagger \frac{(\bar{a}_0^\dagger)^{(N-2)}}{\sqrt{N-2!}} |0\rangle, \\ |\psi_f^{(2)}\rangle = \bar{b}_{\mathbf{k}_0+\mathbf{k}}^\dagger \bar{b}_{\mathbf{k}_0-\mathbf{k}}^\dagger \frac{(\bar{a}_0^\dagger)^{(N-2)}}{\sqrt{N-2!}} |0\rangle. \quad (43)$$

The states are analogous to those in Eq. (35). In particular, $|\psi_i\rangle$ has all particles in a finite-momentum condensate ($\mathbf{k}_0 = [k = k_0, \mathbf{k}_\perp = 0]$).

The scattering rate is then

$$\frac{dN}{dt} = \int \frac{dk}{2\pi} \int \frac{d^2 k_\perp}{(2\pi)^2} |\langle \psi_f^{(1)} | H_{\text{int}} | \psi_i \rangle|^2 \sigma_{12} \\ + \int \frac{dk}{2\pi} \int \frac{d^2 k_\perp}{(2\pi)^2} |\langle \psi_f^{(2)} | H_{\text{int}} | \psi_i \rangle|^2 \sigma_{22}, \quad (44)$$

where

$$\sigma_{12} = \frac{2\pi}{\hbar} \delta \left(\bar{\epsilon}_{k_0-k}^{(1)} + \bar{\epsilon}_{k_0+k}^{(2)} + \frac{(\hbar k_\perp)^2}{m} - 2\bar{\epsilon}_{k_0}^{(1)} \right), \\ \sigma_{22} = \frac{2\pi}{\hbar} \delta \left(\bar{\epsilon}_{k_0-k}^{(2)} + \bar{\epsilon}_{k_0+k}^{(2)} + \frac{(\hbar k_\perp)^2}{m} - 2\bar{\epsilon}_{k_0}^{(1)} \right).$$

In general, $g_{12} = \alpha g_1$ and $g_2 = \beta g_1$. Approximating the Wannier functions with the harmonic oscillator wave functions would yield $\alpha = 1/2$ and $\beta = 3/4$. Rather than using this approximation, we numerically calculate the maximally localized Wannier functions for the experimental lattice depth of $V = 7E_R$ and find that $\alpha = 0.41$ and $\beta = 0.6$.

Extracting the dimensional factors,

$$\tau = \frac{N}{\frac{dN}{dt}} = \frac{2\hbar^3 a}{mg_1^2 n \Gamma}, \quad (45)$$

where the dimensionless parameter Γ depends on the forcing strength and can be expressed as

$$\Gamma = \int \frac{dk}{2\pi} [| -u_{k_0-k} v_{k_0+k} u_{k_0} u_{k_0} + \alpha u_{k_0+k} v_{k_0-k} v_{k_0} v_{k_0} \\ + 2\beta(u_{k_0+k} u_{k_0-k} u_{k_0} v_{k_0} - v_{k_0+k} v_{k_0-k} u_{k_0} v_{k_0})|^2 \\ + [| v_{k_0-k} v_{k_0+k} u_{k_0} u_{k_0} + \alpha u_{k_0+k} u_{k_0-k} v_{k_0} v_{k_0} \\ - 2\beta(v_{k_0+k} u_{k_0-k} u_{k_0} v_{k_0} + u_{k_0+k} v_{k_0-k} u_{k_0} v_{k_0})|^2]. \quad (46)$$

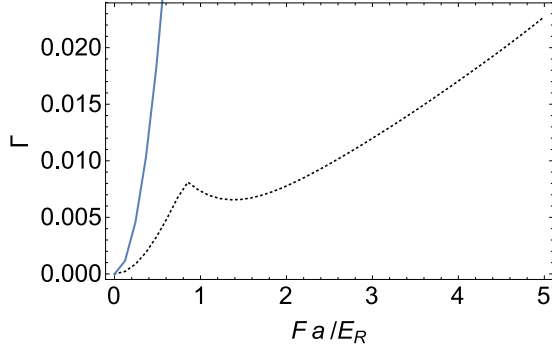


FIG. 3. (Color online) Dimensionless decay rate Γ as a function of amplitude of shaking F for $\omega = 5.5E_R/\hbar$ and $V_0 = 7.0E_R$. The dotted line shows Γ calculated using Eq. (46), while the solid line shows the function $(\frac{F}{\Delta_0})^2$ corresponding to the rate in Eq. (38). The kink shows the paramagnetic-ferromagnetic phase transition.

The dotted line in Fig. 3 shows Γ using $\alpha = 0.41$ and $\beta = 0.6$, corresponding to a lattice depth of $V = 7E_R$. There is a distinct kink in the Γ vs F plot, which shows the paramagnetic-ferromagnetic phase transition. For all F , the numerical calculation gives a smaller Γ than the perturbative estimate in Eq. (37). For the experimental lattice depths, $d \sim 100$ nm, $gn/h \sim 150$ Hz, $a_s \sim 1.5$ nm, yielding $\tau \sim 1$ s which matches experimental observations [20].

IV. GENERAL CONCLUSIONS

A. Form of the scattering rate

Generically, two-particle scattering will give a rate proportional to $g^2 n$. The instabilities studied here relied upon scattering into transverse modes. These rates can be modified by tuning the density of these modes. For example, one could imagine engineering band gaps with transverse optical lattices. Note that such lattices may provide additional confinement and increase the effective g , inadvertently increasing the decay rate.

B. Diffusive dynamics

The same dissipation which causes the condensate to decay can also lead to diffusive motion. Such diffusion may provide another way to study this physics. We model the kinetics by a Boltzmann equation:

$$\frac{\partial n(z, p)}{\partial t} + v(p) \frac{\partial n(z, p)}{\partial z} = \frac{n(z, p) - (n(z)/2\pi)}{\tau}. \quad (47)$$

Here $n(z, p)$ is the coarse-grained number of particles whose position along the lattice direction is z and whose quasimomentum in that direction is p , while $n(z) = \int dp n(z, p)$ is the linear density and the group velocity is $v(p) = \partial \epsilon / \partial p$. We have integrated over the transverse directions. The τ appearing here is exactly the same as in Eqs. (22), (38), and (45). The collision term takes this simple form because atoms are scattered to random values of momentum in the lattice direction after a collision. Taking the zeroth and first moments of the Boltzmann equation yields typical hydrodynamic equations

$$\frac{\partial n(z)}{\partial t} + \frac{\partial J}{\partial z} = 0, \quad (48)$$

$$\frac{\partial J}{\partial t} + \frac{\partial}{\partial z} [\langle v^2 \rangle n(z)] = \frac{J}{\tau}, \quad (49)$$

where the current J is defined by $J = \int dv v(p)n(z, p)$. In the overdamped limit, these can be rewritten as a diffusion equation with diffusion constant $D = \langle v^2 \rangle \tau \propto J_{\text{eff}}^2 \tau$, where J_{eff} is the effective tunneling coefficient [see Eq. (17)]. Observing the diffusive motion may be one way of experimentally measuring τ , complementing more direct methods [64,65].

V. SUMMARY AND OUTLOOK

In this paper we analyzed the stability of a BEC in a driven one-dimensional optical lattice with no transverse confinement. We found that due to the presence of transverse modes, the BEC would always be unstable, and we calculate the decay rates. Experimentally, this instability would be manifest in many forms, including heating and diffusive dynamics. In previous work, we found that in the limit of extremely tight transverse confinement the BEC has regimes of stability.

Generally, experiments are neither in the tight-binding limit nor in the limit with no transverse confinement. The results in the present paper are applicable as long as the level spacing of the quantum modes in the transverse direction (~ 100 Hz for the experiment in Ref. [21]) is small compared to the drive frequency ω (~ 7.3 kHz for the experiment in Ref. [21]). The results from [56] apply in the opposite limit.

ACKNOWLEDGMENTS

We thank the Ketterle group (W. Ketterle, C. J. Kennedy, W. C. Burton, and W. C. Chung) and the Chin group (C. Chin and L. Clark) for correspondence about their experiments. We are particularly indebted to W. Ketterle for suggesting we investigate transverse-mode instabilities. We acknowledge support from the ARO-MURI Non-equilibrium Many-body Dynamics grant (Grant No. W911NF-14-1-0003).

-
- [1] I. M. Georgescu, S. Ashhab, and F. Nori, *Rev. Mod. Phys.* **86**, 153 (2014).
 - [2] J. I. Cirac and P. Zoller, *Nat. Phys.* **8**, 264 (2012).
 - [3] I. Bloch, J. Dalibard, and S. Nascimbéne, *Nat. Phys.* **8**, 267 (2012).
 - [4] R. Blatt and C. F. Roos, *Nat. Phys.* **8**, 277 (2012).
 - [5] A. Aspuru-Guzik and P. Walther, *Nat. Phys.* **8**, 285 (2012).
 - [6] J. Cayssol, B. Dora, F. Simon, and R. Moessner, *Phys. Status Solidi RRL* **7**, 101 (2013).

- [7] E. Arimondo, D. Ciampini, A. Eckardt, M. Holthaus, and O. Morsch, *Adv. At. Mol. Opt. Phys.* **61**, 515 (2012).
- [8] A. Alberti, V. V. Ivanov, G. M. Tino, and G. Ferrari, *Nat. Phys.* **5**, 547 (2009).
- [9] J. Struck, C. Ölschläger, R. Le Targat, P. Soltan-Panahi, A. Eckardt, M. Lewenstein, P. Windpassinger, and K. Sengstock, *Science* **333**, 996 (2011).
- [10] J. Struck, M. Weinberg, C. Olschlager, P. Windpassinger, J. Simonet, K. Sengstock, R. Hoppner, P. Hauke, A. Eckardt, M. Lewenstein, and L. Mathey, *Nat. Phys.* **9**, 738 (2013).
- [11] J. Struck, C. Olschlager, M. Weinberg, P. Hauke, J. Simonet, A. Eckardt, M. Lewenstein, K. Sengstock, and P. Windpassinger, *Phys. Rev. Lett.* **108**, 225304 (2012).
- [12] G. Jotzu, M. Messer, R. Desbuquois, M. Lebrat, T. Uehlinger, D. Greif, and T. Esslinger, *Nature (London)* **515**, 237 (2014).
- [13] M. Aidelsburger, M. Lohse, C. Schweizer, M. Atala, J. T. Barreiro, S. Nascimbéne, N. R. Cooper, I. Bloch, and N. Goldman, *arXiv:1407.4205*.
- [14] C. J. Kennedy, G. A. Siviloglou, H. Miyake, W. C. Burton, and W. Ketterle, *Phys. Rev. Lett.* **111**, 225301 (2013).
- [15] M. Aidelsburger, M. Atala, M. Lohse, J. T. Barreiro, B. Paredes, and I. Bloch, *Phys. Rev. Lett.* **111**, 185301 (2013).
- [16] H. Miyake, G. A. Siviloglou, C. J. Kennedy, W. C. Burton, and W. Ketterle, *Phys. Rev. Lett.* **111**, 185302 (2013).
- [17] A. Alberti, G. Ferrari, V. V. Ivanov, M. L. Chiofalo, and G. M. Tino, *New J. Phys.* **12**, 065037 (2010).
- [18] V. V. Ivanov, A. Alberti, M. Schioppo, G. Ferrari, M. Artoni, M. L. Chiofalo, and G. M. Tino, *Phys. Rev. Lett.* **100**, 043602 (2008).
- [19] H. Miyake, Ph.D. thesis, Massachusetts Institute of Technology, 2013.
- [20] C. V. Parker, L.-C. Ha, and C. Chin, *Nat. Phys.* **9**, 769 (2013).
- [21] L.-C. Ha, L. Clark, C. V. Parker, B. M. Anderson, and C. Chin, *Phys. Rev. Lett.* **114**, 055301 (2015).
- [22] P. Hauke, O. Tielemans, A. Celi, C. Ölschläger, J. Simonet, J. Struck, M. Weinberg, P. Windpassinger, K. Sengstock, and M. Lewenstein, and A. Eckardt, *Phys. Rev. Lett.* **109**, 145301 (2012).
- [23] W. Zheng and H. Zhai, *Phys. Rev. A* **89**, 061603(R) (2014).
- [24] T. Kitagawa, T. Oka, A. Brataas, L. Fu, and E. Demler, *Phys. Rev. B* **84**, 235108 (2011).
- [25] L. Jiang, T. Kitagawa, J. Alicea, A. R. Akhmerov, D. Pekker, G. Refael, J. I. Cirac, E. Demler, M. D. Lukin, and P. Zoller, *Phys. Rev. Lett.* **106**, 220402 (2011).
- [26] Q.-J. Tong, J.-H. An, J. Gong, H.-G. Luo, C. H. Oh, *Phys. Rev. B* **87**, 201109(R) (2013).
- [27] S. K. Baur, M. H. Schleier-Smith, and N. R. Cooper, *Phys. Rev. A* **89**, 051605(R) (2014).
- [28] A. Eckardt and M. Holthaus, *Europhys. Lett.* **80**, 50004 (2007).
- [29] T. Kitagawa, E. Berg, M. Rudner, and E. Demler, *Phys. Rev. B* **82**, 235114 (2010).
- [30] M. Lababidi, I. I. Satija, and E. Zhao, *Phys. Rev. Lett.* **112**, 026805 (2014).
- [31] M. D. Reichl and E. J. Mueller, *Phys. Rev. A* **89**, 063628 (2014).
- [32] C. E. Creffield and F. Sols, *Phys. Rev. A* **90**, 023636 (2014).
- [33] N. Goldman and J. Dalibard, *Phys. Rev. X* **4**, 031027 (2014).
- [34] L. D'Alessio and A. Polkovnikov, *Ann. Phys. (NY)* **333**, 19 (2013).
- [35] L. D'Alessio and M. Rigol, *Phys. Rev. X* **4**, 041048 (2014).
- [36] D. Vorberg, W. Wustmann, R. Ketzmerick, and A. Eckardt, *Phys. Rev. Lett.* **111**, 240405 (2013).
- [37] A. Lazarides, A. Das, and R. Moessner, *Phys. Rev. Lett.* **112**, 150401 (2014).
- [38] A. Lazarides, A. Das, and R. Moessner, *Phys. Rev. E* **90**, 012110 (2014).
- [39] S. De Sarkar, R. Sensarma, and K. Sengupta, *J. Phys. Condens. Matter* **26**, 325602 (2014).
- [40] P. Ponte, A. Chandran, Z. Papić, and D. A. Abanin, *Ann. Phys. (NY)* **353**, 196 (2015).
- [41] W. Zheng, B. Liu, J. Miao, C. Chin, and H. Zhai, *Phys. Rev. Lett.* **113**, 155303 (2014).
- [42] M. Bukov, L. D'Alessio, and A. Polkovnikov, *arXiv:1407.4803*.
- [43] A. Eckardt, C. Weiss, and M. Holthaus, *Phys. Rev. Lett.* **95**, 260404 (2005).
- [44] Á. Gómez-León and G. Platero, *Phys. Rev. Lett.* **110**, 200403 (2013).
- [45] A. G. Grushin, Á. Gómez-León, and T. Neupert, *Phys. Rev. Lett.* **112**, 156801 (2014).
- [46] E. Suárez Morell and L. E. F. Foa Torres, *Phys. Rev. B* **86**, 125449 (2012).
- [47] P. M. Perez-Piskunow, G. Usaj, C. A. Balseiro, and L. E. F. Foa Torres, *Phys. Rev. B* **89**, 121401(R) (2014).
- [48] N. H. Lindner, G. Refael, and V. Galitski, *Nat. Phys.* **7**, 490 (2011).
- [49] N. H. Lindner, D. L. Bergman, G. Refael, and V. Galitski, *Phys. Rev. B* **87**, 235131 (2013).
- [50] Y. T. Katan and D. Podolsky, *Phys. Rev. Lett.* **110**, 016802 (2013).
- [51] D. E. Liu, A. Levchenko, and H. U. Baranger, *Phys. Rev. Lett.* **111**, 047002 (2013).
- [52] A. Kundu and B. Seradjeh, *Phys. Rev. Lett.* **111**, 136402 (2013).
- [53] T. Bilitewski and N. R. Cooper, *arXiv:1410.5364*.
- [54] N. Goldman, J. Dalibard, M. Aidelsburger, and N. R. Cooper, *arXiv:1410.8425*.
- [55] R. Citro, E. G. Dalla Torre, L. D'Alessio, A. Polkovnikov, M. Babadi, T. Oka, and E. Demler, *arXiv:1501.05660*.
- [56] S. Choudhury and E. J. Mueller, *Phys. Rev. A* **90**, 013621 (2014).
- [57] C. E. Creffield, *Phys. Rev. A* **79**, 063612 (2009).
- [58] O. Júrgensen, F. Meinert, M. J. Mark, H.-C. Nägerl, and D.-S. Lühmann, *Phys. Rev. Lett.* **113**, 193003 (2014).
- [59] O. Morsch, J. H. Müller, M. Cristiani, D. Ciampini, and E. Arimondo, *Phys. Rev. Lett.* **87**, 140402 (2001).
- [60] K. R. A. Hazzard and E. J. Mueller, *Phys. Rev. A* **81**, 033404 (2010).
- [61] A. R. Kolovsky, H. J. Korsch, and E.-M. Graefe, *Phys. Rev. A* **80**, 023617 (2009).
- [62] D. J. Berkeland, J. D. Miller, J. C. Bergquist, W. M. Itano, and D. J. Wineland, *J. Appl. Phys.* **83**, 5025 (1998).
- [63] A. Verdeny, A. Mielke, and F. Mintert, *Phys. Rev. Lett.* **111**, 175301 (2013).
- [64] U. Schneider, L. Hackermüller, J. P. Ronzheimer, S. Will, S. Braun, T. Best, I. Bloch, E. Demler, S. Mandt, D. Rasch, and A. Rosch, *Nat. Phys.* **8**, 213 (2012).
- [65] J. P. Ronzheimer, M. Schreiber, S. Braun, S. S. Hodgman, S. Langer, I. P. McCulloch, F. Heidrich-Meisner, I. Bloch, and U. Schneider, *Phys. Rev. Lett.* **110**, 205301 (2013).